Title: Concise syntheses of GB22, GB13 and himgaline by cross-coupling and complete reduction

Authors: Eleanor M. Landwehr,[1,†] Meghan A. Baker,[1,†,‡] Takuya Oguma,[1,†,§] Hannah E. Burdge,[1,¶] Takahiro Kawajiri,[1,§] Ryan A. Shenvi[1,*]

Affiliations:

[1]Department of Chemistry, Scripps Research, La Jolla, United States.

Present Address:

[‡]Merck & Co., South San Francisco, United States

[§]Shionogi & Co., Ltd., Toyonaka, Japan

[¶]Pfizer, Inc., La Jolla, United States

[*]Corresponding author: rshenvi@scripps.edu

[†]These authors contributed equally to this work.

Abstract: Neuroactive metabolites from the bark of *Galbulimima belgraveana* occur in variable distribution among trees and are not easily procured by chemical synthesis due to elaborate bond networks and dense stereochemistry. Previous syntheses of complex congeners like himgaline have relied on iterative, stepwise installation of multiple methine stereocenters. Here we decrease the synthetic burden of himgaline to nearly one-third of the prior best (7–9 vs. 19–31 steps) by cross-coupling high fraction aromatic (F_{Ar}) building blocks followed by complete, stereoselective reduction to high-fraction sp^3 (F_{sp^3}) products. This short entry into GB alkaloid space allows its extensive exploration and biological interrogation.

One-Sentence Summary: Aromatic building blocks are merged and reduced stereoselectively to yield surprising syntheses of complex plant metabolites.

Main Text: Extracts from *Galbulimima belgraveana* and *baccata* have yielded related neuroactive alkaloids *(1,2)* classified by connectivity between piperidine and decalin domains (GB alkaloids, classes I–IV, Fig. 1A and 1B) *(3).* Different connectivity and substitution patterns confer diverse and profound biological effects in mammals *(2)*, but only a single target has been defined. The simplest, class I GB alkaloid, himbacine (15 mcbits/atom) *(4),* was found to antagonize muscarinic receptors $M_{1–5}$ (rhodopsin-like GPCRs, subfamily A18) *(5,6).* Its enantiomeric series was developed by total synthesis into Vorapaxar, an antagonist of related GPCR PAR-1 (subfamily A15) *(7),* establishing important precedent for perturbation of selectivity among metabotropic receptors with medicinal potential. Whereas class I alkaloids effect bradycardia and putative psychotropic activity in mice, class II alkaloids cause tachycardia and hypotension, and class III alkaloids like himgaline (**1**) are antispasmodic (class IV alkaloids have not been assayed) *(2)*. One or more components of *G. belgraveana* bark cause hallucination in humans, but a psychotropic principle has not been identified *(1).* Aside from himbacine, the remaining 39 alkaloids have not been well-developed towards biological goals, obstructed by the alkaloid content in bark—a mixture of more than thirty congeners that varies unpredictably from 0.5% to only trace amounts *(8)*—and synthetic intractability *(3).* This compound problem of poor material access, absence of target annotation and translational potential of multiple bioactive metabolites has attracted significant interest from the synthesis community *(3,9–14).* GB alkaloid classes II and III have proved especially challenging to access (18–33 steps), although pioneering solutions have appeared (see Supplementary Materials Fig. S1–7 for a full outline of each) *(9–14).* The most concise syntheses by Movassaghi *(10),* Sarpong *(13)* and Ma *(14)* obtained GB13 in 18–19 steps, and generated crucial data to aid our exploration.

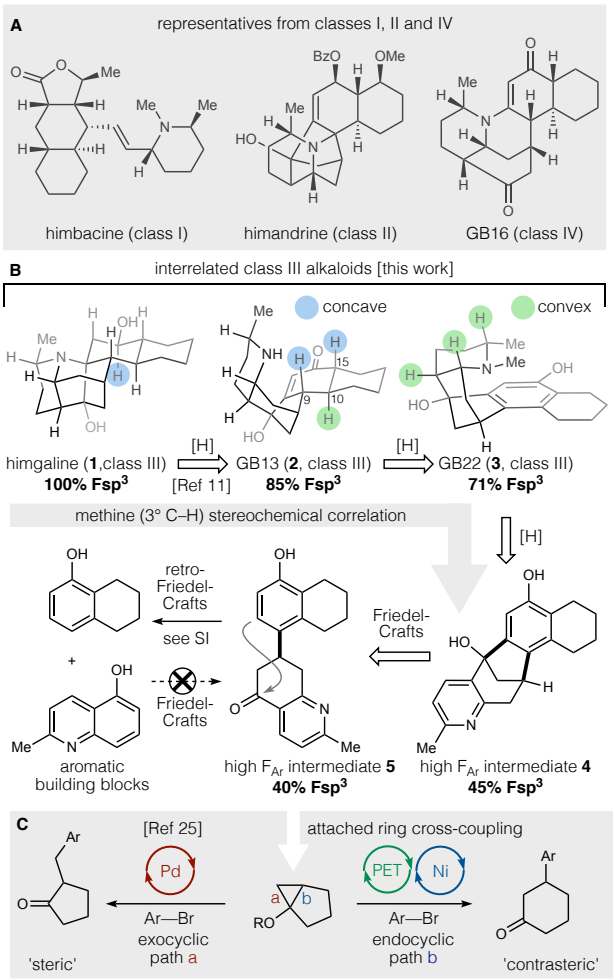

Fig. 1. Representative *Galbulimima* (GB) alkaloids and synthetic analysis. (**A**) Chemical space related to GB alkaloids. (**B**) Through-class retrosynthetic analysis relating GB alkaloids. (**C**) A high F_{Ar}, low $F_{sp}3$ intermediate undergoes rapid attached ring scission, but can be formed under mild cross-coupling conditions.

In search of a general strategy to access GB alkaloid chemical space, we targeted GB22 (**3**, Fig. 1B) *(15)*, a low-abundance class III alkaloid (1.8 ppm, milled bark) whose aromatic ring might allow rapid entry and diversification to complex congeners. In this design, high fraction aromatic (F_{Ar}) intermediate **5** containing 15 sp^2 atoms (11 mcbits/atom) might be reduced *(13,16)* to generate the 11 tetrahedral stereocenters in the complex alkaloid himgaline (**1**, 21 mcbits/atom). This is a classical strategy, represented by the earliest alkaloid synthesis—coniine in 1886—in which reduction converted a simple aromatic to a high F_{sp^3} alkaloid, albeit with one stereocenter whose stereochemistry was not controlled *(17)*. Success in himgaline would require relay of stereochemical configuration from the single stereocenter of **5** to nine prochiral carbons, including the concave-facing methine C–H bonds of GB13 (**2**). Although these hydrogens might epimerize to the concave face, the potential instability of extended enols and the existence of other low-energy configurations at ring junctions complicated our analysis of stereochemical equilibration (e.g. 9,10,15-*epi*-GB13 and 15-*epi*-GB13 are 2.6 kcal/mol and 1.3 kcal/mol lower in energy than GB13; see Fig. S8–10). Here we report unusually concise syntheses of GB22, GB13 and himgaline

using an *endo*-selective attached-ring cross-coupling and arene reduction that significantly reduce the synthetic burden compared to prior art.

Retrosynthetic analysis of GB22 (Fig. 1B) identified an embedded attached-ring system, which could be unmasked by pyridine hydrogenation *(13)* and intramolecular ketone arylation transforms. Despite the simplicity of **5**, the most obvious disconnection—enone conjugate addition—fails. A direct Friedel-Crafts addition of **4** into the cyclohexadienone conjugate acid of **3** (Fig. 2A) *(18)* is prevented by preferential protonation of **4** and decomposition of **5** mediated by acids (see below). We thought that if the oxocarbenium ion were replaced with a β-keto carbon-centered radical, we might circumvent the Friedel-Crafts by interception of an arylnickel complex (Fig. 2C) *(19)*. β-Keto radical formation has been implicated in the ring-opening of siloxycyclopropanes by photoinduced electron transfer (PET) to 1,4-dicyanonaphthalene (DCN) *(20)*. Inspired by the recent success of photoredox/Ni dual catalytic cross-coupling platforms *(21),* we considered a system in which a photoexcited catalyst might oxidatively cleave a siloxycyclopropane with *endo*-selectivity *(22,23,24),* leading to arylnickel capture and reductive elimination. Typically, transition-metal catalyzed arylations of cyclopropanols and siloxycyclopropanols favor cleavage of the least hindered cyclopropane bond (path a, Fig. 1C) *(25)*. In contrast, this electron transfer arylation would provide the opposite regioselectivity (path b).

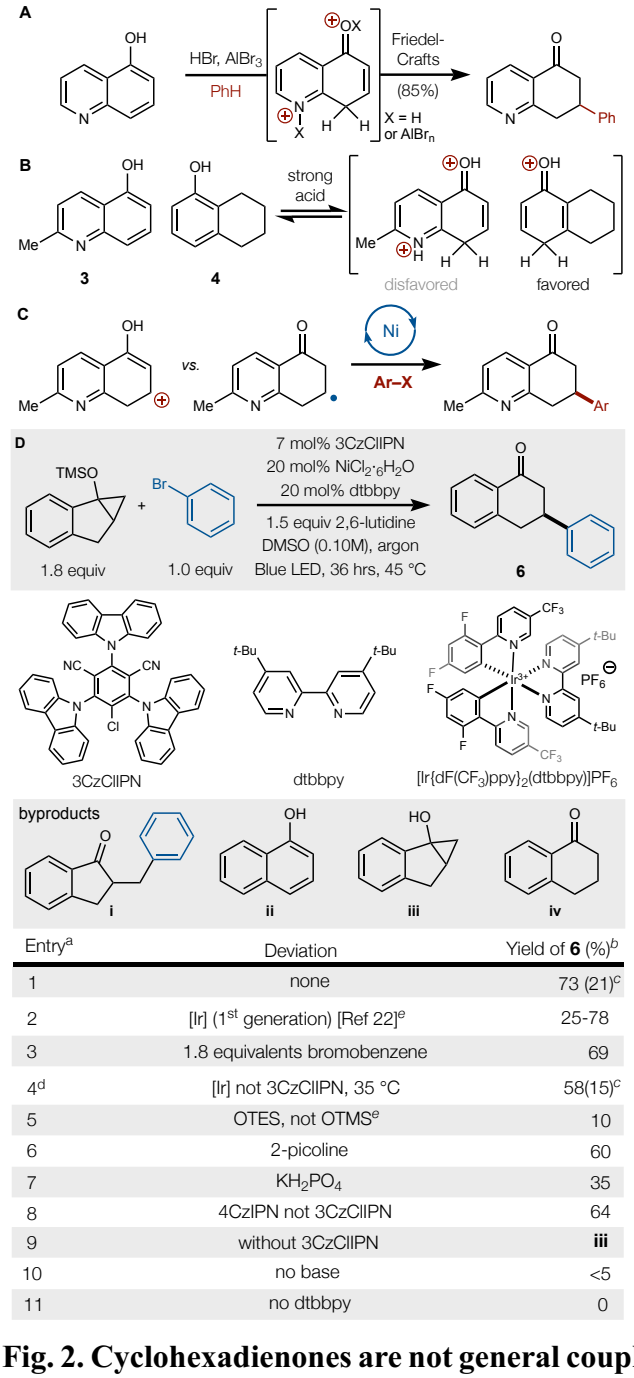

Entry[a]	Deviation	Yield of **6** (%)[b]
1	none	73 (21)[c]
2	[Ir] (1st generation) [Ref 22][e]	25-78
3	1.8 equivalents bromobenzene	69
4[d]	[Ir] not 3CzClIPN, 35 °C	58(15)[c]
5	OTES, not OTMS[e]	10
6	2-picoline	60
7	KH_2PO_4	35
8	4CzIPN not 3CzClIPN	64
9	without 3CzClIPN	**iii**
10	no base	<5
11	no dtbbpy	0

Fig. 2. Cyclohexadienones are not general coupling partners. (**A**) The failure of a Friedel-Crafts conjugate arylation. (**B**) Acids disfavor protonation of 5-quinolol. (**C**) Conceptual replacement of the cationic intermediate with a β-keto or -enol radical leads to the development of the corresponding cross-coupling. (**D**) Optimization substrates and results. [a]0.1 mmol bromobenzene, [b]^{1}H NMR yield, [c](%yield of **i**), [d]0.25 mmol bromobenzene. [e]with [Ir].

Early efforts to develop a dual catalytic *endo*-selective siloxycyclopropane arylation identified the Doyle-MacMillan dual catalyst system of [Ir{dF(CF$_3$)ppy}$_2$(dtbbpy)]PF$_6$ and Ni(dtbbpy)Cl$_2$ as a good starting point (see Fig. 2D) *(26)*. Yields of coupled product **6** proved dependent on heat removal by air circulation and difficult to reproduce without tight control of temperature (**ii**–**iv**,

Fig. 2D, were major byproducts). Ultimately, the reaction setup was altered to accommodate the use of a water bath for temperature control and heating. In combination with organic dyes like 3CzClIPN and 4CzIPN, the reaction proved more reliable and offered shorter reaction times, lower costs and more flexibility over conditions *(27)*. Highly-polar solvents such as DMA and DMF were competent in this chemistry, but DMSO out-performed both. Additionally, carbonate bases were ineffective and phosphate bases proved inferior and less consistent than organic pyridine bases like 2,6-lutidine and 2-picoline. The yield of **6** decreased when we employed photocatalysts that had higher or lower oxidation potentials than 3CzClIPN. Finally, the reaction did not proceed in control reactions that excluded each of the reagents (see Tables S1–S4). These conditions were generally successful across a variety of siloxycyclopropanes and haloarenes (Fig. 3A). In all cases, the retrosynthetic disconnections using a conjugate addition transform would lead to a cyclohexadienone that exists as the phenol tautomer (**ii**).

Neither electron-withdrawing nor electron-donating groups on the arene effected the efficiency of coupling and heterocycles coupled with efficiency (oxidant-sensitive arenes were problematic, however; see pages S20–S31). The reaction translated from bromoarenes to 1-bromocyclohexene, albeit in reduced yield. Encouraged by the scope of this cross-coupling, especially with regard to heterocyclic substrates, we investigated entry into the synthesis of GB22 (Fig. 3B). Ketone **7** is listed commercially and can be prepared in one step by condensation of 1,3-cyclopentanedione, methyl vinyl ketone, and ammonia *(28)*. Conversion to siloxycyclopropane **8** was carried out *via* silyl enol ether formation, followed by Simmons-Smith cyclopropanation using the Shi modification *(29)*. An alternative 3-step route to **8** from methyl 2-chloro-6-methyl-nicotinate was also developed to avoid the difficult purifications of the Simmons-Smith route. Cross-coupling with bromoarene **9a** or **9b** (2 steps from 1-naphthol) *(30)* occurred cleanly, after optimization to account for *ortho*-substitution that leads to steric crowding of the intermediate arylnickel (see Tables S6–S9). The higher yield of anisole **9b** likely reflects the low bond dissociation enthalpy of C–H bonds in benzyl ether **9a**.

The high F_{Ar} attached-ring intermediates **10a**/**b** incorporated all the skeletal carbons of GB22, GB13 and himgaline, but the projected Friedel-Crafts arylation proved difficult. First, as suggested by positive Hammett parameters *(31),* dominant inductive effects disfavor attack by the *meta*-position of the phenolic ether. Koltunov found benzene itself to cyclize efficiently with 5-quinolol using triflic acid (F_3CSO_3H) *(18)* but initial screens of strong Brønsted acids in our system delivered only small quantities of **4**. Triflic acid instead competitively protonated **10a**/**b** and effected a retro-Friedel-Crafts arylation to cleave the hard-won C–C bond and return quinolol **3** (see Fig. 1B and Table S5). Typical Lewis acids like $AlCl_3$ also did not yield **11**. However, when inorganic aluminum Lewis acids were mixed with hexafluoroisopropanol (HFIP), tetracycle **4** was finally observed, albeit in low yield, along with **3**. We suspect that an aluminum species such as $Al[OCH(CF_3)_2]_nCl_m$ might act as an efficient Lewis acid *(32)* or hydrogen-bonding catalyst. Minimization of strong Brønsted acidity (i.e. HCl liberation) was accomplished by adding diethylaluminium chloride to HFIP, which quickly and exothermically evolved gas (likely ethane) to generate a new complex, tentatively assigned as $Al[OCH(CF_3)_2]_2Cl$ and its aggregates. The mechanism of cyclization may involve acidification of HFIP, formation of a strong double hydrogen-bond donor bridged by aluminum, or formation of a strongly Lewis acidic complex *(33)* HFIP alone *(34)* did not promote any reaction of **2**. This procedure led to clean and reproducible cyclization of the acid-labile attached ring as either the parent phenol **4** (52%) or its methyl ether **11** (86%), depending on use of **10a** (to **4**) or **10b** (to **11**).

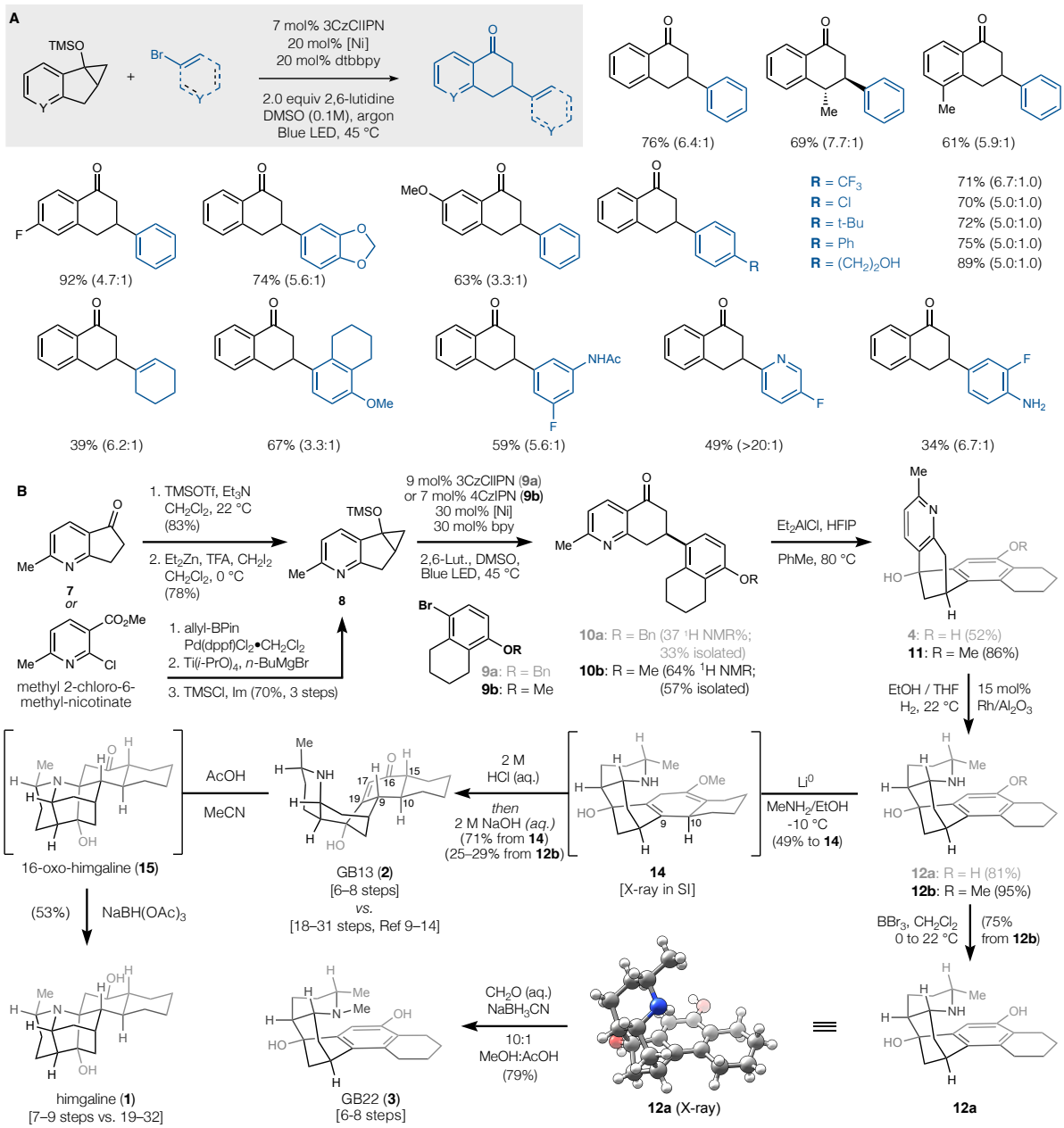

Fig. 3. Scope and application. (**A**) *Endo*-selective sp^3-sp^2 cross-coupling: % isolated yield (*endo*:*exo*). (**B**) A short synthesis of GB22, GB13 and himgaline via iterative, stereoselective reduction of multiple correlated carbons.

Both **4** and **11** could be hydrogenated over Rh/Al_2O_3 with exquisite stereocontrol to **12a**/**b** (other diastereomers not detected), by analogy to related work on GB13 wherein a larger, pre-saturated decalin motif provided steric shielding *(13)*. Here, the benzene nucleus was unaffected by rhodium-catalyzed hydrogenation, but despite its planarity, small size and ability to adsorb to metal surfaces *(35)* it efficiently blocked the concave face of the pyridine ring. Whereas **12a** could be *N*-methylated (CH_2O (aq.), $NaCNBH_3$) to GB22 directly, **12b** required demethylation by BBr_3 (75%), resulting in one more operation than the benzyl ether series, but almost double the yield

(16% vs. 29%, 3 vs. 4 steps). ^{1}H- and ^{13}C-NMR spectra of synthetic GB22 were identical to those reported by Lan and Mander (see page S119) *(15)*.

The next arene reduction benefited from retention of the methyl ether in **12b** and probed the role of the piperidine ring in control of stereochemistry at the incipient decalone. Birch reduction (Li^0 or Na^0 in NH_3 (l)) and electrochemical reduction proved unsuccessful, but Benkeser reduction *(36)* (Li^0 in $MeNH_2$, THF/*i*-PrOH) was unique to effect clean reduction of the anisole. Proton source and metal proved crucial: MeOH, EtOH and *t*-BuOH did not promote reduction, and neither was Na^0 effective. The recently reported Koide reduction *(37)* (Li^0, ethylenediamine, THF) worked extremely well and yielded similar amounts of product to $Li^0/MeNH_2$ with greater operational ease. A single diastereomer and regioisomer predominated (**14**, for X-ray structure see Fig. S11), resulting from intermolecular protonation of C10 from the convex face, despite the potential for intramolecular proton transfer to C9 from the piperidine N–H, modeled only 2.46Å apart in **12a** (X-ray). Minor byproduct pathways included demethylation (to **12a**), over-reduction of the arene and *ca.* 10% of a regioisomer. Hydrolysis of **14** with 2M aqueous HCl, followed by basification (4M NaOH) led to GB13 in 71% yield, with each of the remaining methine stereocenters adopting the desired configuration. Only a single methine (C10) positioned its hydrogen to the convex face, whereas two new stereocenters (C9, C15) derived from prochiral, planar carbons that projected hydrogens *inward*. This stereochemistry may reflect, in part, the thermodynamic preferences of ring-tautomer (aza-Michael product) 16-oxo-himgaline (**15**), which forms spontaneously under acidic conditions *(11)*. Whereas the decalin *cis*-ring fusion of GB13 is calculated to be more stable by 1.3 kcal/mol, the *trans*-ring fusion of 16-oxo-himgaline is lower in energy by 2.7 kcal/mol (see Fig. S8–10). We speculate that the piperidine ammonium may deliver a proton internally to the enone γ-carbon C9 since β,γ to α,β-enone isomerization occurs under acidic conditions and an extended enol tautomer is occluded on its concave face by this ammonium (see **14** X-ray, Fig. S12). The final stereogenic methine C–H was installed according to a one-step protocol, as first demonstrated in a 33-step synthesis of himgaline *(12)*. Thus, 9 prochiral carbons of high F_{Ar} intermediate **10b** was converted in 3 steps to 9 new stereocenters (8 carbon, 1 nitrogen) by relay of increasing stereochemical information through simple reductions. To access pure GB13, **14** can be chromatographed to remove reduction byproducts prior to acid hydrolysis, but this is unnecessary for conversion to pure himgaline, resulting in a 7–9 step synthesis, depending on isolation of **14** and designation of official starting material (**7** *vs*. cyclopentane-1,3-dione *vs*. methyl 2-chloro-6-methyl-nicotinate, see Fig. 4).

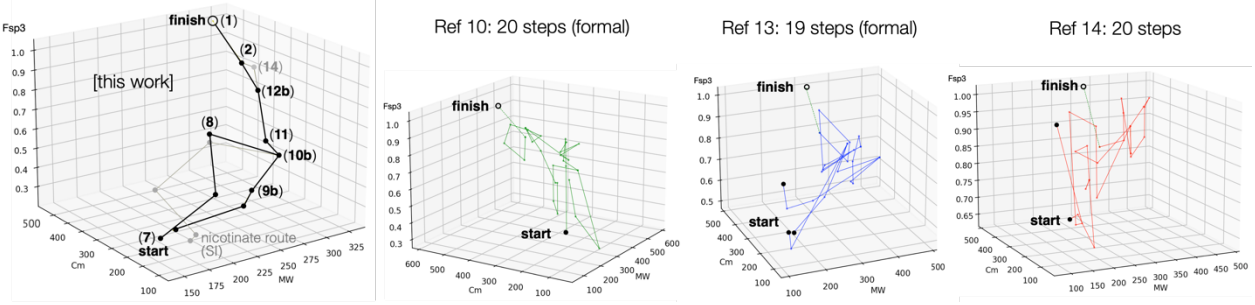

Fig. 4. Himgaline syntheses as walks through a chemical space parameterized by F_{sp^3} ($\#C_{sp^3}/C_{total}$), C_m (mcbit) and molecular weight (Da).

Himgaline is constitutionally related to cross-coupled product **10b** by these iterative additions of H_2, excluding the *O*-methyl embedded in starting material **9b**. Since hydrogen atoms are

typically omitted from complexity calculations *(38),* the progression of high F_{Ar} intermediates to 100% F_{sp^3} (himgaline) is exclusively due to information carried by molecular topology (C–C, C–N, C–O bonds) and chirality content. Here, the 260.16 mcbits *(4)* of *des*-methyl **10b** increase to 477.83 over 5 steps, or 43.5 mcbits per step. Visualized as a walk through chemical space *(39)* (Fig. 4), the synthesis begins proximal to commercial space (low molecular weight, low complexity and low F_{sp^3} /high F_{Ar}), converges early by cross-coupling and then rapidly reaches the high complexity, weight and F_{sp^3} of himgaline, typical of remote GB alkaloid space. In contrast, the shortest prior synthesis of himgaline (formal, racemic, 19 steps) varies 148.45 mcbits over 15 steps (9.9 mcbits per step) from the latest point of convergency. Each route allows its own unique exploration of different areas of chemical space. However, recognition that the key methine C–H stereocenters can be stereoselectively appended from prochiral sp^2 carbons of an aromatic himgaline core simplifies access to GB alkaloid space in a clear and quantifiable way. Whereas this analysis focuses on navigation to high complexity chemotypes, we anticipate that GB structural chemical space can be better parameterized to relate to the biological targets and relative potencies among family members. With this goal in mind, we have scaled cross-coupling to 1.3 g of **10b**, the Friedel-Crafts to 1 g of **11** and the hydrogenation to 834 mg of **12b** for diversification and target identification. Given the structural similarity among the 25 class II and III congeners, this approach is likely to prove general and finally provide a means to deconvolute the targets, functions and translational potential of the GB alkaloids.

References and Notes:

(1) B. Thomas, Psychoactive plant use in Papua New Guinea: a review. *Science in New Guinea*. **25**, 33–59 (2000).

(2) D. J. Collins, C. C. J. Culvenor, J. A. Lamberton, J. W. Loder, J. R. Price, "Pharmacology of alkaloids" in *Plants for Medicines* (Commonwealth Scientific and Industrial Research Organization (CSIRO), Melbourne, 1990), pp. 71–106.

(3) U. Rinner, "Galbulimima alkaloids" in *The Alkaloids: Chemistry and Biology* (Elsevier, Amsterdam), vol. 78, chap. 2.

(4) T. Böttcher, An Additive Definition of Molecular Complexity. *J. Chem. Inf. Model.* **56**, 462–470 (2016).

(5) A. H. Gilani, L. B. Cobbin, Interaction of himbacine with carbachol at muscarinic receptors of heart and smooth muscle. *Arch. Int. Pharmacodyn. Ther.* **290**, 46–53 (1987).

(6) J. H. Miller, P. J. Aagaard, V. A. Gibson, M. McKinney, Binding and Functional Selectivity of Himbacine for Cloned and Neuronal Muscarinic Receptors. *J. Pharmacol. Exp. Ther.* **263**, 663–667 (1992).

(7) S. Chackalamannil, Y. Wang, W. J. Greenlee, Z. Hu, Y. Xia, H. S. Ahn, G. Boykow, Y. Hsieh, J. Palamanda, J. Agans-Fantuzzi, S. Kurowski, M. Graziano, M. Chintala, Discovery of a Novel, Orally Active Himbacine-Based Thrombin Receptor Antagonist (SCH 530348) with Potent Antiplatelet Activity. *J. Med. Chem.* **51**, 3061–3064 (2008).

(8) S. Binns, P. J. Dunstan, G. B. Guise, G. M. Holder, A. F. Hollis, R. S. McCredie, J. T. Pinhey, R. H. Prager, M. Rasmussen, E. Ritchie, W. C. Taylor, The Chemical Constituents of *Galbulimima* species. *Aust. J. Chem.* **18**, 569–573 (1965).

(9) L. N. Mander, M. M. McLachlan, The Total Synthesis of the Galbulimima Alkaloid GB 13. *J. Am. Chem. Soc.* **125**, 2400–2401 (2003).

(10) M. Movassaghi, D. K. Hunt, M. Tjandra, Total Synthesis and Absolute Stereochemical Assignment of (+)- and (-)-Galbulimima Alkaloid 13. *J. Am. Chem. Soc.* **128**, 8126–8127 (2006).
(11) U. Shah, S. Chackalamannil, A. K. Ganguly, M. Chelliah, S. Kolotuchin, A. Buevich, A. McPhail, Total Synthesis of (−)-Himgaline. *J. Am. Chem. Soc.* **128**, 12654–12655 (2006).
(12) D. A. Evans, D. J. Adams, Total Synthesis of (+)-Galbulimima Alkaloid 13 and (+)-Himgaline. *J. Am. Chem. Soc.* **129**, 1048–1049 (2007).
(13) K. K. Larson, R. Sarpong, Total Synthesis of Alkaloid (±)-G.B. 13 Using a Rh(I)-Catalyzed Ketone Hydroarylation and Late-Stage Pyridine Reduction. *J. Am. Chem. Soc.* **131**, 13244–13245 (2009).
(14) W. Zi, S. Yu, D. A. Ma, Convergent Route to the Galbulimima Alkaloids (-)-GB 13 and (+)-GB 16. *Angew. Chem. Int. Ed.* **49**, 5887–5890 (2010).
(15) P. Lan, A. J. Herlt, A. C. Willis, W. C. Taylor, L. N. Mander, Structures of New Alkaloids from Rain Forest Trees *Galbulimima belgraveana* and *Galbulimima baccata* in Papua New Guinea, Indonesia, and Northern Australia. *ACS Omega,* **3**, 1912–1921 (2018).
(16) E. R. Welin, A. Ngamnithiporn, M. Klatte, G. Lapointe, G. M. Pototschnig, M. S. J. McDermott, D. Conklin, C. D. Gilmore, P. M. Tadross, C. K. Haley, E. Glibstrup, C. U. Grünanger, K. M. Allan, S. C. Virgil, D. J. Slamon, B. M. Stoltz, Concise total syntheses of (–)-jorunnamycin A and (–)-jorumycin enabled by asymmetric catalysis. *Science* **363**, 270–275 (2019).
(17) A. Ladenburg, Synthese der activen Coniine. *Ber. Dtsch. Chem. Ges*. **19**, 2578−2583 (1886).
(18) K. Y. Koltunov, G. K. S. Prakash, R. Rasul, G. A. Olah, Reactions of 5-, 6-, 7-, 8-Hydroxyquinolines and 5-Hydroxyisoquinoline with Benzene and Cyclohexane in Superacids. *J. Org. Chem.* **67**, 4330–4336 (2002).
(19) S. A. Green, J. L. M. Matos, A. Yagi, R. A. Shenvi, Branch-Selective Hydroarylation: Iodoarene-Olefin Cross Coupling. *J. Am. Chem. Soc.* **138**, 12779–12782 (2016).
(20) H. Rinderhagen, P. A. Waske, J. Mattay, Facile ring opening of siloxy cyclopropanes by photoinduced electron transfer. A new way to β-keto radicals. *Tetrahedron* **62**, 6589–6593 (2006).
(21) G. Molander, J. A. Milligan, J. P. Phelan, S. O. Badir, Recent Advances in Alkyl Carbon-Carbon Bond Formation by Nickel/Photoredox Cross-Coupling. *Angew. Chem., Int. Ed.* **58**, 6152–6163 (2019).
(22) H. E. Burdge, T. Oguma, T. Kawajiri, R. A. Shenvi, Concise synthesis of GB22 by *endo*-selective siloxycyclopropane arylation. *ChemRxiv* DOI: 10.26434/chemrxiv.8263415.v1
(23) N. Varabyeva, M. Barysevich, Y. Aniskevich, A. Hurski, $Ti(OiPr)_4$-Enabled Dual Photoredox and Nickel-Catalyzed Arylation and Alkenylation of Cyclopropanols. *Org. Lett.* **23**, 5452–5456 (2021).
(24) D. D. Bume, C. D. Pitts, T. Lectka, Tandem C–C Bond Cleavage of -Cyclopropanols and Oxidative Aromatization by Manganese(IV) Oxide in a Direct C–H to C–C Functionalization of Heteroaromatics. *Eur. J. Org. Chem.* **2016**, 26–30 (2016).
(25) S. Aoki, T. Fujimura, E. Nakamura, I. Kuwajima, Palladium-Catalyzed Arylation of Siloxycyclopropanes with Aryl Triflates. Carbon Chain Elongation via Catalytic Carbon-Carbon Bond Cleavage. *J. Am. Chem. Soc.* **110**, 3296–3298 (1988).

(26) Z. Zuo, D. T. Ahneman, L. Chu, J. A. Terrett, A. G. Doyle, D. W. C. MacMillan, Merging photoredox with nickel catalysis: Coupling of α-carboxyl sp^3-carbons with aryl halides. *Science* **345**, 437–440 (2014).

(27) E. Speckmeier, T. G. Fischer, K. A. Zeitler, Toolbox Approach to Construct Broadly Applicable Metal-Free Catalysts for Photoredox Chemistry: Deliberate Tuning of Redox Potentials and Importance of Halogens in Donor−Acceptor Cyanoarenes. *J. Am. Chem. Soc.* **140**, 15353–15365 (2018).

(28) C. Allais, F. Liéby-Muller, J. Rodriguez. T. Constantieux, Metal-Free Michael-Addition-Initiated Three-Component Reaction for the Regioselective Synthesis of Highly Functionalized Pyridines: Scope, Mechanistic Investigations and Applications. *Eur. J. Org. Chem.* **2013**, 4131–4145 (2013).

(29) J. C. Lorenz, J. Long, Z. Yang, S. Xue, Y. Xie, Y. Shi, A Novel Class of Tunable Zinc Reagents ($RXZnCH_2Y$) for Efficient Cyclopropanation of Olefins. *J. Org. Chem.* **69**, 327–334 (2004).

(30) J. A. Lowe, W. Qian, S. E. Drozda, R. A. Volkmann, D. Nason, R. B. Nelson, C. Nolan, D. Liston, K. Ward, S. Faraci, K. Verdries, Structure−Activity Relationships of Potent, Selective Inhibitors of Neuronal Nitric Oxide Synthase Based on the 6-Phenyl-2-aminopyridine Structure. *J. Med. Chem.* **47**, 1575–1586 (2004).

(31) C. Hansch, A. Leo, Substituent Constants for Correlation Analysis in Chemistry and Biology. Wiley-Interscience, NY, 1979.

(32) K. S. Mazdiyasni, B. J. Schaper, L. M. Brown, Hexafluoroisopropoxides of Aluminum and of Some Group IV Elements. *Inorg. Chem.* **10**, 889–892 (1971).

(33) H. Yamamoto, K. Futasuta, 'Designer Acids': Combined Acid Catalysis for Asymmetric Synthesis. *Angew. Chem. Int. Ed.* **44**, 1924–1942 (2005).

(34) H. F. Motiwala, R. H. Vekariya, J. Aubé, Intramolecular Friedel−Crafts Acylation Reaction Promoted by 1,1,1,3,3,3-Hexafluoro-2-propanol. *Org. Lett.* **17**, 5484−5487 (2015).

(35) S. Mitsui, S. Imaizumi, Y. Esashi, Stereochemistry and Mechanism of Catalytic Hydrogenation and Hydrogenolysis. III. Catalytic Hydrogenolysis of Benzyl-type Alcohols and Their Derivatives. *Bull. Chem. Soc. Jpn.* **43**, 2143 – 2152 (1970).

(36) R. A. Benkeser, C. Arnold Jr. R.F. Lambert, O. H. Thomas, Reduction of organic compounds by lithium in low molecular weight amines. III. Reduction of aromatic compounds containing functional groups. *J. Am. Chem. Soc.* **77**, 6042–6045 (1955).

(37) J. Burrows, S. Kamo, K. Koide, Scalable Birch reduction with lithium and ethylenediamine in tetrahydrofuran. *Science* **374**, 741–746 (2021)

(38) S. H. Bertz, The First General Index of Molecular Complexity. *J. Am. Chem. Soc.* **103**, 3599−3601 (1981).

(39) R. M. Demoret, M. A. Baker, M. Ohtawa, S. Chen, C.-C. Lam, S. Khom, M. Roberto, S. Forli, K. Houk, R. A. Shenvi, Synthetic, Mechanistic and Biological Interrogation of *Ginkgo biloba* Chemical Space en route to (–)-Bilobalide. *J. Am. Chem. Soc.* **142**, 18599–18618 (2020).

(40) M. S. Lowry, J. I. Goldsmith, J. D. Slinker, R. Rohl, R. A. Pascal, G. G. Malliaras, S. Bernhard, Single-Layer Electroluminescent Devices and Photoinduced Hydrogen Production from an Ionic Iridium(III) Complex. *Chem. Mater.* **2005**, *17*, 5712-5719.

(41) J. A. Walker, K. L. Vickerman, J. N. Humke, L. M. Stanley, Ni-Catalyzed Alkene Carboacylation via Amide C-N Bond Activation. *J. Am. Chem. Soc.* **2017,** *139*, 10228-10231.

(42) M. Uyanik, T. Yasui, K. Ishihara, Hydrogen Bonding and Alcohol Effects in Asymmetric Hypervalent Iodine Catalysis: Enantioselective Oxidative Dearomatization of Phenols. *Angew. Chem. Int. Ed.* **2013**, 52, 9215-9218.
(43) E. F. Pettersen, T. D. Goddard, C. C. Huang, G. S. Couch, D. M. Greenblatt, E. C. Meng, T. E. Ferrin, UCSF Chimera--a visualization system for exploratory research and analysis. *J. Comput. Chem.* **2004** *25*, 1605–1612.

Acknowledgements. We thank Leo Smith (Concordia College, Moorhead) for assistance with the synthesis of **8** and Sarah Jane Hill for assistance with Matplotlib. We thank Professor Nathan Jui for sending 3D-printed racks for photochemical reactions and Cheng Bi for help with high pressure hydrogenation. We thank Professor Hans Renata and Dr. Steven Crossley for proofreading. Arnold Rheingold, Milan Gembicky and Erika Samolova are thanked for X-ray crystallographic analysis.

Funding
National Institutes of Health grant GM122606 (RAS)
National Science Foundation grant CHE1856747 (RAS)
Skaggs Graduate School fellowship (EML)
Bristol Myers Squibb fellowship (MAB)
Jiangsu Industrial Technology Research Institute (JITRI) fellowship (MAB, HEB)
Shionogi & Co., Ltd. fellowship (TO)
Japan Society for the Promotion of Science (JSPS) fellowship 17J08551 (TK)

Author contributions RAS directed the research. HEB devised first-generation conditions for cross-coupling; EML and MAB devised second-generation conditions. TO developed the synthesis of **3**, MAB, RAS and EML developed conditions for reduction of **12b** and EML completed, optimized, and scaled syntheses of **1** and **2**. EML and RAS parameterized Ref. 9–14 as walks through a chemical space. RAS, EML and MAB composed the manuscript and the Supplementary Materials section.

Competing interests: A provisional patent has been filed.

Data and materials availability: All data is made available in the main text or the Supplementary Materials, including experimental procedures, copies of NMR spectra, X-ray structure reports and full outlines of prior syntheses. Structural parameters for X-ray crystal structures are available from the Cambridge Crystallographic Data Centre (**12a**: CCDC 2122295; **14**: 2123248). Coordinates and Matplotlib Python code are included in the same Supporting Materials file as the experimental procedures.

Supplementary Materials:
References 40–43 are cited only in the SM.
Figures S1–S7 depict syntheses from Ref. 9–14 in identical schematic formats.
Figures S8–S10 depict molecular models and relative energies of GB13 and 16-oxo-himgaline diastereomers.
Figures S11–S12 display X-ray structures for **12b** and **14**, respectively.
Tables S1–S4, S6–9 show variations in cross-coupling conditions.
Table S5 shows variations in Friedel-Crafts conditions.
Table S10 is a comparison between himgaline synthesized here and in Ref. 11.